GLIA 45:354–363 (2004)

Electrophysiological and Molecular Evidence of L-(Ca_v1), N- ($Ca_v2.2$), and R- ($Ca_v2.3$) Type Ca^{2+} Channels in Rat Cortical Astrocytes

MARCELLO D'ASCENZO,[1] MAURO VAIRANO,[2] CATIA ANDREASSI,[3] PIERLUIGI NAVARRA,[2] GIAN BATTISTA AZZENA,[1] AND CLAUDIO GRASSI[1]*

[1]*Institute of Human Physiology, Medical School, Catholic University "S. Cuore," Rome, Italy*
[2]*Institute of Pharmacology, Medical School, Catholic University "S. Cuore," Rome, Italy*
[3]*Institute for Clinical Neurobiology, Bayerische Julius-Maximilians-Universität, Würzburg, Germany*

KEY WORDS rat cortical astrocytes; Ca_v1; $Ca_v2.2$; $Ca_v2.3$; high-voltage-activated Ca^{2+} channels; α_1 subunit transcripts; RT-PCR; patch-clamp

ABSTRACT Changes in intracellular Ca^{2+} levels are an important signal underlying neuron-glia cross-talk, but little is known about the possible role of voltage-gated Ca^{2+} channels (VGCCs) in controlling glial cell Ca^{2+} influx. We investigated the pharmacological and biophysical features of VGCCs in cultured rat cortical astrocytes. In whole-cell patch-clamp experiments, L-channel blockade (5 μM nifedipine) reduced Ba^{2+} current amplitude by 28% of controls, and further decrease (32%) was produced by N-channel blockade (3 μM ω-conotoxin-GVIA). No significant additional changes were observed after P/Q channel blockade (3 μM ω-conotoxin-MVIIC). Residual current (36% of controls) amounted to roughly the same percentage (34%) that was abolished by R-channel blockade (100 nM SNX-482). Electrophysiological evidence of L-, N-, and R-channels was associated with RT-PCR detection of mRNA transcripts for VGCC subunits α_{1C} (L-type), α_{1B} (N-type), and α_{1E} (R-type). In cell-attached recordings, single-channel properties (L-currents: amplitude, -1.21 ± 0.02 pA at 10 mV; slope conductance, 22.0 ± 1.1 pS; mean open time, 5.95 ± 0.24 ms; N-currents: amplitude, -1.09 ± 0.02 pA at 10 mV; slope conductance, 18.0 ± 1.1 pS; mean open time, 1.14 ± 0.02 ms; R-currents: amplitude, -0.81 ± 0.01 pA at 20 mV; slope conductance, 10.5 ± 0.3 pS; mean open time, 0.88 ± 0.02 ms) resembled those of corresponding VGCCs in neurons. These novel findings indicate that VGCC expression by cortical astrocytes may be more varied than previously thought, suggesting that these channels may indeed play substantial roles in the regulation of astrocyte Ca^{2+} influx, which influences neuron-glia cross-talk and numerous other calcium-mediated glial-cell functions.

INTRODUCTION

There is increasing evidence that astrocytes play a fundamental role in brain function by signaling to neurons and influencing their activity. These glial cells can affect the development of synaptic contacts among neurons as well as the latter's ability to process information (Araque et al., 1999; Parpura and Haydon, 2000; Ullian et al., 2001). Synaptic efficiency is influenced by glial-cell sequestration of neurotransmitters present in the synaptic cleft and their subsequent liberation through various mechanisms, including calcium-dependent release (Attwell, 1994; Parpura et al., 1994;

Grant sponsor: Ministero dell'lstruzione, dell'Universitá e della Ricerca (MIUR); Grant sponsor: Catholic University "S. Cuore."

*Correspondence to: Claudio Grassi, Institute of Human Physiology, Medical School, Catholic University "S. Cuore," Largo F. Vito 1, 00168 Rome, Italy. E-mail: grassi@rm.unicatt.it

Received 6 August 2003; Accepted 17 September 2003

DOI 10.1002/glia.10336

Pfrieger and Barres, 1997; Bezzi et al., 1998; Araque et al., 2000). Changes in intracellular Ca^{2+} concentrations are in fact the key signal for cross-talk between astrocytes and neurons (Haydon, 2001). Astrocyte Ca^{2+} concentrations are reportedly increased by glutamate and a number of other neurotransmitters, including ATP, GABA, noradrenaline, and acetylcholine (Cornell-Bell et al., 1990; Verkhratsky et al., 1998; Haydon, 2001; Latour et al., 2001). They can also be modified by the second messenger inositol-1,4,5-triphosphate (IP_3), which induces Ca^{2+} release from intracellular stores (Leybaert et al., 1998).

While the importance of these mechanisms to astrocyte Ca^{2+} homeostasis is well established, less attention has been paid to the potential contribution of Ca^{2+} influx through voltage-gated Ca^{2+} channels (VGCCs). The electrophysiological characterization of VGCC currents in these cells is also far from complete. The few studies conducted to date have demonstrated the presence of low-voltage-activated (T-type) channels and high-voltage-activated (HVA) dihydropiridine-sensitive (L-type) channels (MacVicar and Tse, 1988; Barres et al., 1989), but much less is known about the other types of HVA Ca^{2+} channels. Moreover, the biophysical properties of astrocyte VGCCs have never been studied at the single-channel level.

In the present study, we used electrophysiological recordings of macroscopic and unitary currents and molecular assays for α_1-subunit transcripts to identify the types of functionally operative VGCCs present in rat cortical astrocytes. In addition to occasional low-voltage-activated (LVA) T-type currents, we recorded currents flowing through HVA L-, N-, and R-type Ca^{2+} channels, but there was no evidence of significant P/Q channel activity. At the molecular level, however, transcripts were found for α_1 subunits corresponding to all four HVA channel types, including the P/Q type. The single-channel properties of the Ca_v1 (L-type), $Ca_v2.2$ (N-type), and $Ca_v2.3$ (R-type) currents, which have never been investigated in glial cells, resemble those of the corresponding channels found in neurons. These findings indicate that VGCCs may be expected to play significant functional roles in the control of cortical astrocyte Ca^{2+} influx and, consequently, in the calcium-mediated glial cell functions.

MATERIALS AND METHODS

Cell Cultures

Primary cultures of rat cortical astrocytes were prepared according to the procedures reported by McCarthy and De Vellis (1980) with minor modifications, as previously described (Vairano et al., 2002). Briefly, 1- to 2-day-old Wistar rats were decapitated, and their brains were rapidly removed under aseptic conditions and placed in phosphate-buffered saline (PBS) with Ca^{2+} and Mg^{2+} containing 100 IU/ml penicillin and 100 μg/ml streptomycin (Sigma Chemical, St. Louis, MO). The cortex was dissected, cut into small fragments, and digested with 0.125% trypsin (Biochrom, Berlin, Germany) in 10 ml PBS without Ca^{2+} and Mg^{2+} (PBS-wo) for 25 min at 37°C. Single cells were then obtained by mechanical dissociation in Dulbecco's MEM with glutamax-I (DMEM; Gibco, Life Technologies, Paisley, U.K.) containing 10% heat-inactivated endotoxin-free fetal calf serum (FCS; Gibco). The same batch of FCS was used for all the astrocyte cultures used in the present study. Cells were seeded at a density of $1.0–1.5 \times 10^7$ cells/10 ml in 75 cm^2 flasks and incubated at 37°C in a humidified atmosphere containing 5% CO_2. The culture medium was changed within 24 h of seeding and twice a week thereafter. When the astrocytes had formed a monolayer firmly attached to the bottom of the flask (8–9 days after dissection), the culture medium was replaced with PBS-wo, and the flasks were vigorously shaken to remove the oligodendrocytes and microglia growing as nonadherent cells on the astrocyte monolayer. Astrocytes were then detached from the flask by a 5-min 0.05% trypsin-EDTA treatment (Euroclone) and subcultured twice at intervals of 7–9 days, i.e., the average time needed for cells to reach confluence. The second subculture was grown in the 35 mm Petri dishes used for patch-clamp experiments. The average total time from dissection to experiments was 28 days. The purity of the astrocyte culture was assessed by flow cytometry as previously reported (Vairano et al., 2002), and it was never lower than 95%. The absence of neuronal contamination was further confirmed by RT-PCR analysis with primers for the astrocyte marker, glial fribillary acidic protein (GFAP), and the neuron-specific SNAP-25 gene.

Macroscopic Current Recordings

Macroscopic Ba^{2+} currents were recorded using the patch-clamp technique in whole-cell or perforated-patch configurations (Hamill et al., 1981) with an Axopatch 200B amplifier (Axon Instruments, Union City, CA). Electrodes were fabricated from thin-wall borosilicate glass capillaries (Clark Electromedical Instruments, Pangbourne Reading, U.K.) using a model P-97 Flaming-Brown micropipette puller (Sutter Instrument, Novato, CA) and fire-polished on a microforge (Narishige Scientific Instrument, Tokyo, Japan). The final resistance of the electrode filled with the standard internal solution described below was 3–5 MΩ. Stimulation and data acquisition were performed with the Digidata 1200 series interface and pCLAMP 6.0.3 software (Axon Instruments). Currents were filtered at 5 kHz with an eight-pole low-pass filter. Capacitative transient and leakage currents were compensated online using the clamp-amplifier settings and offline by subtraction of Cd^{2+}-insensitive (200 μM Cd^{2+}) currents.

Before electrophysiological recordings, the culture medium was removed and replaced with Tyrode's solution containing (in mM) 150 NaCl, 4 KCl, 2 $MgCl_2$, 2 $CaCl_2$, 10 glucose, and 10 4-(2-hydroxyethyl)-piperazineethanesulphonic acid (HEPES); pH was adjusted

to 7.4 with NaOH. The external solution was (in mM) 125 NaCl, 10 $BaCl_2$, 1 $MgCl_2$, 10 HEPES, and 0.0001 tetrodotoxin (TTX) to block Na^+ currents; pH was adjusted to 7.3 with NaOH. The standard internal solution for whole-cell recordings contained (in mM) 110 CsCl, 10 tetraethylammonium chloride (TEA-Cl), 2 $MgCl_2$, 10 ethylenebis(oxonitrilo)tetraacetate (EGTA), 8 glucose, 10 HEPES, and, to minimize current rundown during experiments, 4.0 adenosine 5′-triphosphate (ATP) magnesium salt, 0.25 adenosine 3′,5′-cyclic monophosphate (cAMP) sodium salt, and 4.0 phosphocreatine disodium salt; pH was adjusted to 7.3 with CsOH.

For perforated-patch recordings, the pipette tip was filled with internal solution containing (in mM) 135 $CsMeSO_3$, 8 NaCl, 2 $MgCl_2$, and 20 HEPES (pH 7.3 with CsOH). The electrode was then back-filled with the same solution with the addition of 50–100 μg/ml amphotericin B from stock aliquots (50 mg/ml in dimethyl sulfoxide) stored at −20°C. Current recording was started when the access resistance decreased below 15 MΩ, which usually occurred within 10 min of sealing (Rae et al., 1991).

Solutions containing the different test agents were exchanged by means of a perfusion system consisting of a multibarreled pipette placed within 100 μm of the patched cell and connected to different syringes by means of Teflon tubes. The gravity-regulated flow rate, 0.3–0.5 ml/min, allowed complete renewal of the extracellular environment in less than 1 s. The cell membrane was depolarized every 10 s (pulse duration, 120–200 ms) at voltages ranging from −40 to 50 mV from the holding potential (V_h) of −90 mV. To isolate HVA currents, each depolarizing pulse was preceded by a 40-ms pulse at −40 mV, which is normally sufficient for complete inactivation of LVA (T-type) Ca^{2+} channels. Unless otherwise specified, the data presented below refer to the effects of test agents on Ba^{2+} currents elicited by depolarization at 0 mV. Current density (pA/pF) was estimated by dividing current amplitude by membrane capacitance, measured by the C_{slow} compensation setting of the patch-clamp amplifier.

Single-Channel Recordings

Unitary activity of HVA Ca^{2+} channels was recorded in the cell-attached configuration. Electrodes were pulled from thick borosilicate glass capillaries (Hilgenberg, Mansfield, Germany) and coated with Sylgard 184 (Dow-Corning, Midland, MI). Their final resistance after filling with the recording solution was 4–9 MΩ. The pipette solution contained (in mM) 100 $BaCl_2$, 10 TEA-Cl, 1 $MgCl_2$, 10 Na-HEPES, and 0.0003 TTX (pH adjusted to 7.3 with TEAOH). Membrane potential was zeroed by perfusing the cell with a control solution containing (in mM) 135 KAsp, 1 $MgCl_2$, 10 HEPES, 5 EGTA, and 0.0003 TTX (pH adjusted to 7.3 with KOH). In experiments performed to study L-channel activity, 10 μM ω-conotoxin-MVIIC (CTx-MVIIC; Tocris Cookson, Bristol, U.K.) and 5 μM (−)-Bay K 8644 (Sigma) were added to the pipette solution, and depolarizing stimuli ranging from 0 to 20 mV were applied from V_h = −40 mV. When N-channels were studied, the internal solution contained 5 μM nifedipine (Sigma) and 100 nM SNX-482 (Peptide Institute, Osaka, Japan), and the cell membrane was depolarized to 10–30 mV from V_h = −80 mV. Unitary R-channel activity was recorded in cells pretreated for 10 min with Tyrode's solution containing 3 μM ω-conotoxin-GVIA (CTx-GVIA; Alomone, Jerusalem, Israel) and 10 μM CTx-MVIIC. Nifedipine (5 μM) and CTx-MVIIC (10 μM) were also added to the pipette solution, and depolarizing steps ranging from 10 to 30 mV were applied from V_h = −80 mV. Pulse duration was 120–500 ms for studies of all channel types. Nifedipine and Bay K 8644 were diluted before each experiment from 1 mM stock solutions in ethanol, which were stored in the dark at 4°C.

Current traces were acquired at 10 kHz and filtered online at 2 kHz. Data were analyzed with TAC and TACFIT software (version 3.04; Bruxton, Seattle, WA). Fast capacitative transients were minimized online by patch-clamp analogue compensation. Uncorrected capacitative currents were eliminated by averaging sweeps with no channel activity (nulls) and subtracting them from each active sweep. Event detection was performed with the 50% threshold detection method, and each transition was visually inspected before being accepted.

Histograms representing open times were plotted on square root-log coordinates and constructed as previously described (Carabelli et al., 2002; D'Ascenzo et al., 2002). Data were not corrected for missed events, and the distributions of open times were fitted with the sum of decaying exponentials. The mean amplitude of the unitary current was determined by fitting the amplitude histograms with a Gaussian distribution. Unitary conductance was evaluated by linear regression of mean unitary currents recorded at voltages ranging from 0 to 20 mV for L-channels and from 10 to 30 mV for N- and R-channels.

All patch-clamp experiments were performed at room temperature (22–24°C). Data are presented as mean ± SEM. Student's *t*-test was used for statistical analysis, and *P* values smaller than 0.05 were considered significant.

RT-PCR

Total RNA was isolated from astrocyte cell cultures or rat brain tissue using the Trizol Reagent (Life Technologies), and 2 μg of RNA were used for cDNA synthesis using the Superscript First-Strand Synthesis System (Invitrogen, Paisley, U.K.) according to the manufacturer's instructions. Twenty nanograms of cDNA were then used as a template for amplification in a reaction mixture containing 400 nM of each primer, 1.5 mM magnesium, and 1.5 U Taq. Primer sequences were as follows: α_{1A}

forward, 5′-CGAGAACAGCCTTATCGTCAC-3′, α_{1A} reverse, 5′-GTGGAGAGGATGAACATGGAGC-3′ (product size, 260 bp); α_{1B} forward, 5′-GGTGAAAGCACAGAGCTTCTACTG-3′, α_{1B} reverse, 5′-CCAACAGAGCGAAGACCACAATG-3′ (product size, 445 bp); α_{1C} forward, 5′-GGAGCTGGACAAGGCTATGAAG-3′, α_{1C} reverse, 5′-GACCTAGAGAGGCAGAGCGAAG-3′ (product size, 652 bp); α_{1D} forward, 5′-TACATGCTCTGTGCGTTCCTG-3′, α_{1D} reverse, 5′-CGATCGTGGTGTTCTTCGCAG-3′ (product size, 573 bp); α_{1E} forward 5′-GCTATCGCTGTGGACAATCTCG-3′, α_{1E} reverse, 5′-TAGTGGCAAGCCTTGCGGATCG-3′ (product size, 1,348 bp); SNAP-25 forward, 5′-GAGGACGCAGACATGCGTAATG-3′, SNAP-25 reverse, 5′-GTCCAACAACATTGGAGGAGAG-3′ (product size, 654 bp); GFAP forward, 5′-GAGTCTCATGGACGGCACAGAC-3′; GFAP reverse, 5′-CAGGACTGCCTTAGTGGCCATTC-3′ (product size, 381 bp); actin forward, 5′-GTGGGCCGCCCTAGGCACCAG-3′; actin reverse, 5′-CTCTTTAATGTCACGCACGATTTC-3′ (product size, 539 bp). After a denaturation step of 5 min at 94°C, the amplification was carried out at 94°C for 30 s, 58°C for 30 s, and 72°C for 1 min for 45 cycles. As a control, cDNA from the same preparations was subjected to 30 cycles of PCR with primers for β-actin. All PCR products were resolved on 1.5% agarose gel. As a positive control, amplification reactions were performed on cDNA prepared from brain tissue and, as negative control, on astrocyte samples without previous reverse transcription.

RESULTS

Identification of L-, N-, and R-Type Ca^{2+} Channels in Rat Cortical Astrocytes

In the first group of experiments, macroscopic Ba^{2+} currents were recorded to verify the presence of functioning VGCCs on the plasma membranes of cortical astrocytes and to characterize pharmacologically the channel types generating these currents. In some experiments, the perforated-patch configuration was preferred over the whole-cell configuration since it allowed greater recording stability over time. Since data obtained with the two configurations were not significantly different, they were pooled.

During depolarizing pulses at 0 mV from V_h of −90 mV, Ba^{2+} currents of variable amplitude were found in 54 out of 93 (58%) cells (Fig. 1). Current density varied widely from cell to cell (range, 3–45 pA/pF). The delivery of 40-ms pulses at −40 mV prior to test depolarization occasionally revealed currents flowing through the LVA (T-type, Ca_v3) Ca^{2+} channels (Fig. 1A).

We then focused our attention on identifying the different types of HVA channels expressed on the astrocyte cell membrane. Application of 5 μM nifedipine, which blocks dihydropiridine-sensitive L-type channels (Ca_v1), reduced the peak-current amplitude by 28.3% ± 4.5% compared with controls (n = 48; Fig. 2). The effect of nifedipine was not homogeneous: marked differences were noted among the different astrocyte

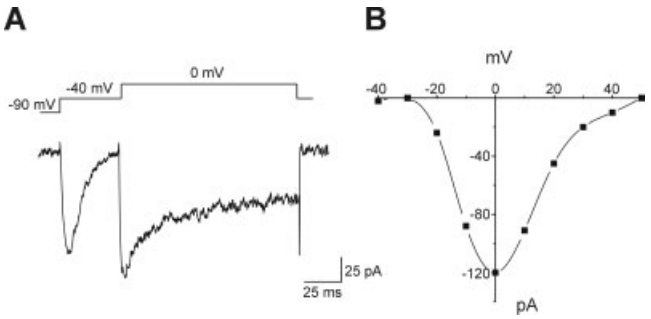

Fig. 1. Macroscopic Ba^{2+} currents in rat cortical astrocytes. **A:** Representative trace showing low-voltage- and high-voltage-activated currents elicited by step depolarization at 0 mV preceded by a 40-ms prepulse at −40 mV from V_h = −90 mV. **B:** Current-to-voltage relationship of the HVA currents recorded from the same cell shown in A.

preparations, and some variability was also observed among cells within the same culture dish. Two different astrocyte subpopulations could therefore be distinguished based on functional L-channel expression: in the first (25% of all cells studied) L-currents accounted for almost three-fourths of total HVA current (74.5% ± 5.3%; n = 12), while their contribution was much more limited (13.0% ± 2.3% of controls; n = 36) in the second group (75% of the tested cells). In the presence of nifedipine, the selective blocker of N-type Ca^{2+} channels, CTx-GVIA (3 μM), further reduced the HVA current by 32.3% ± 5.8% of controls (n = 7). The subsequent application of 3 μM CTx-MVIIC did not significantly diminish the HVA current (2.3% ± 0.9% reduction), suggesting that, under our experimental conditions, P/Q channels do not contribute to Ca^{2+} influx into cortical astrocytes. The residual current (36.5% ± 6.2%) that was resistant to nifedipine, CTx-GVIA, and CTx-MVIIC was abolished by 200 μM Cd^{2+}. In another group of experiments, a similar percentage of total HVA current (34.2% ± 3.6%; n = 11) was abolished by the selective R-channel blocking agent SNX-482 (100 nM; Fig. 2C).

Single-Channel Parameters

Our macroscopic current recordings demonstrated that L-, N-, and R-type Ca^{2+} channels are indeed present and functionally active on the plasma membranes of cortical astrocytes. To gain more information on the biophysical properties of these channels, we recorded unitary VGCC activity in cell-attached patches. As noted above, for L-channel recordings, 10 μM CTx-MVIIC and 5 μM Bay K 8644 were added to the pipette solution. In some experiments, recordings were also made with Bay K 8644 in the external zeroing solution instead of the internal solution. At the end of successful recordings, the solution containing Bay K 8644 was replaced with the same zeroing solution containing 5 μM nifedipine. Disappearance of channel activity in the latter condition provided further evidence that the recorded channels were indeed L-type.

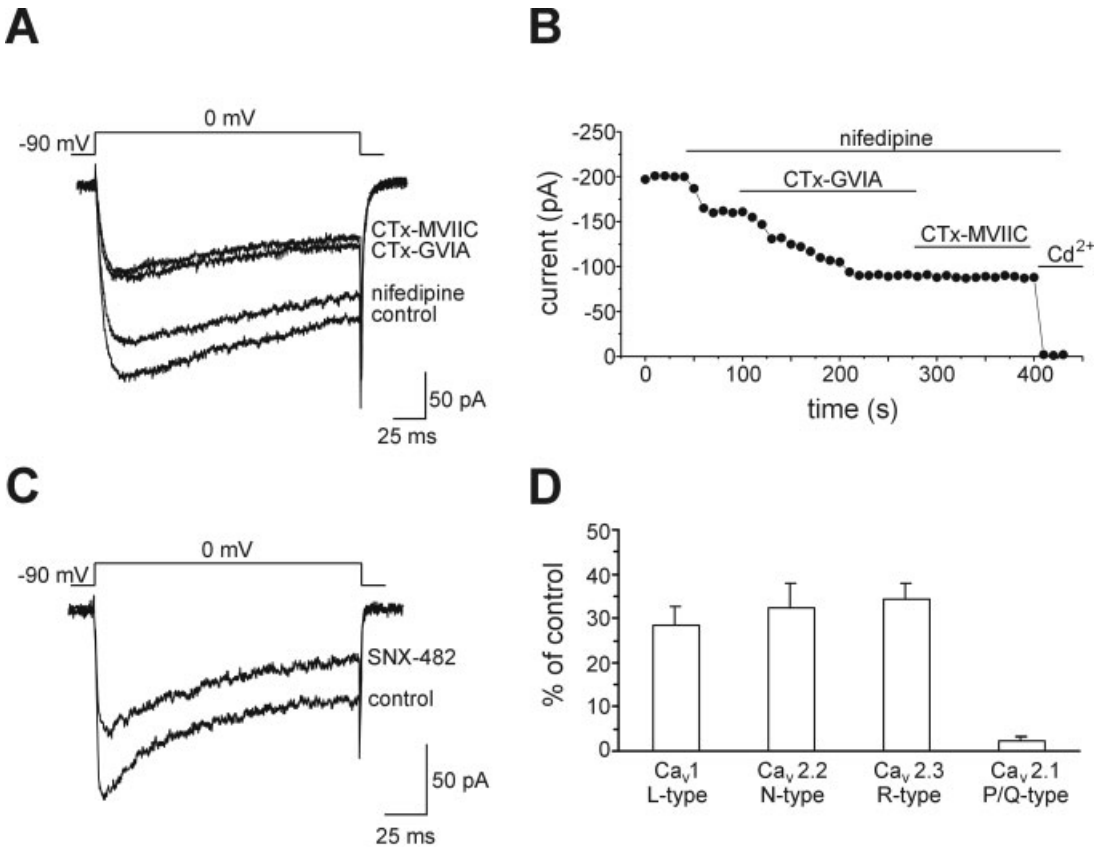

Fig. 2. Pharmacological characterization of different HVA currents in rat cortical astrocytes. **A:** HVA currents recorded before (control) and after application of 5 μM nifedipine (which blocks L-type channels), 3 μM CTx-GVIA (blockade of N-type channels), and 3 μM CTx-MVIIC (P/Q channel blockade). **B:** Time plot of data from the experiment shown in A and blockade of residual current (i.e., resistant to L-, N-, and P/Q channel blockade) by 200 μM Cd^{2+}. **C:** Reduction of HVA current by the selective blocker of R-type channels SNX-482 (100 nM). **D:** Percent contributions of the different types of VGCCs to the total HVA current recorded in cortical astrocytes.

Figure 3 shows representative traces of L-channel activity in cortical astrocytes during depolarization at 10 mV from $V_h = -40$ mV (Fig. 3A) and the amplitude distribution at 10 mV (mean, -1.21 ± 0.02 pA; n = 8; Fig. 3B). Current amplitudes were -1.41 ± 0.03 (n = 7) and -0.97 ± 0.02 (n = 9) at 0 and 20 mV, respectively, and slope conductance (obtained by plotting data collected at 0, 10, 20 mV) was 22.0 ± 1.1 pS. The open time distribution at 10 mV was fitted with one exponential function with $\tau_o = 5.60$ ms. Similar results were obtained when mean open time was calculated as the arithmetic mean of all data (5.95 ± 0.24 ms).

In another group of experiments, N-channel activity was recorded during depolarization steps ranging from 10 to 30 mV from $V_h = -80$ mV. Pipette solutions contained 5 μM nifedipine and 100 nM SNX-482. Channel conductance, evaluated by measuring current amplitudes at voltages ranging from 10 to 30 mV, was 18.0 ± 1.1 pS (Fig. 4). Current amplitude was -1.09 ± 0.02 pA at 10 mV (n = 6), -0.89 ± 0.02 pA at 20 mV (n = 7), and -0.73 ± 0.02 pA at 30 mV (n = 4). Plots of the open time distribution at 20 mV were fitted according to one exponential function with $\tau_o = 1.04$ ms. Arithmetic mean of open times was 1.14 ± 0.02 ms when all data from seven patches were pooled.

For recordings of unitary R-channel activity, we used the same stimulation protocol employed for N-channel recordings; the pipette solution contained 5 μM nifedipine and 10 μM CTx-MVIIC. Prior to recording, the cells were treated for 10 min with Tyrode's solution containing 3 μM CTx-GVIA and 10 μM CTx-MVIIC. Figure 5 shows representative traces of R-channel activity and current amplitude distribution at 20 mV with mean value of -0.81 ± 0.01 pA (n = 4). Current amplitudes were -0.92 ± 0.01 (n = 4) and -0.71 ± 0.01 pA (n = 3) at 10 and 30 mV, respectively, and slope conductance was 10.5 ± 0.3 pS. The open time distribution at 20 mV was fitted with one exponential having $\tau_o = 0.80$ ms. Mean open time calculated as the arithmetic mean of all data was 0.88 ± 0.02 ms.

Expression of VGCC α_1 Subunits in Cultured Astrocytes

Total RNA extracted from cultured astrocytes was subjected to RT-PCR analysis to determine whether transcripts for VGCC α_1 subunits paralleled the HVA channel subtype profiles obtained in electrophysiological studies. To exclude the risk of false positive results

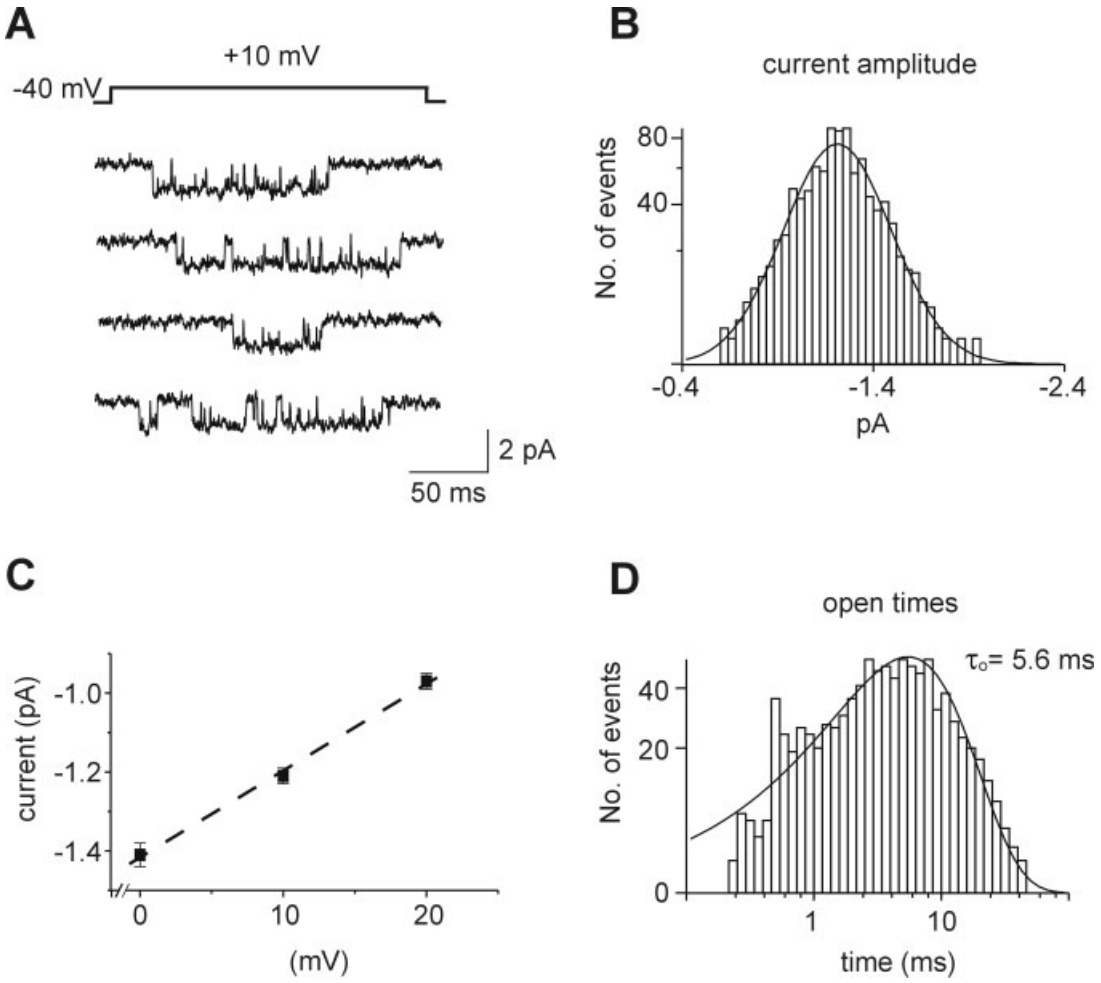

Fig. 3. Biophysical properties of L-type Ca^{2+} channels recorded from cell-attached patches. **A:** Representative traces of L-channel activity during depolarization at 10 mV from $V_h = -40$ mV. Pipette solution contained 10 μM CTx-MVIIC and 5 μM Bay K 8644. **B:** Distribution of L-current amplitudes at 10 mV. **C:** Slope conductance of L-channel measured by plotting current amplitudes at 0, 10, and 20 mV. **D:** Distribution of N-channel open times at 10 mV.

related to neuronal contamination of the astrocyte cultures, we first tested the purity of the culture through amplification of the glial marker GFAP and the neuronal marker SNAP-25. Primers for SNAP-25 amplification were selected from a region of the sequence showing no homology with that of the astroglial gene SNAP-23 (Latour et al., 2003). As shown in Figure 6, only amplification of the glial marker GFAP was observed.

The same samples were then used in different PCR assays with primers specific for the different classes of Ca^{2+} channels. Expression of subunits α_{1A} (P/Q type), α_{1B} (N-type), α_{1C} (L-type), and α_{1E} (R-type) was readily detected, but there was no evidence of α_{1D} subunit expression, even after reamplification of the RT-PCR product. Finally, amplification of β-actin transcript was performed as a loading control.

DISCUSSION

Data reported in the present study provide electrophysiological evidence that different types of HVA Ca^{2+} channels are present and functionally operating on the membrane of rat cortical astrocytes. L- (Ca_v1), N- ($Ca_v2.2$), and R- ($Ca_v2.3$) type channels were identified by pharmacological characterization of macroscopic currents, and their biophysical properties were defined by single-channel recordings. Numerous studies, based primarily on immunostaining, fluorescence, or molecular biology techniques, have demonstrated VGCC expression on the cell membranes of cultured astrocytes (Verkhratsky and Steinhäuser, 2000; Latour et al., 2003). Other reports, however, indicate that this expression is absent under physiological conditions (Carmignoto et al., 1998) and stressed its role in the pathophysiology of brain injury (Westenbroek et al., 1998; Agrawal et al., 2000; Chung et al., 2001).

The existence of VGCCs in astrocytes and glial cells in general has also been demonstrated in electrophysiological studies (MacVicar, 1984; Barres et al., 1989; MacVicar et al., 1991; Verkhratsky and Steinhäuser, 2000). However, these studies mostly revealed the

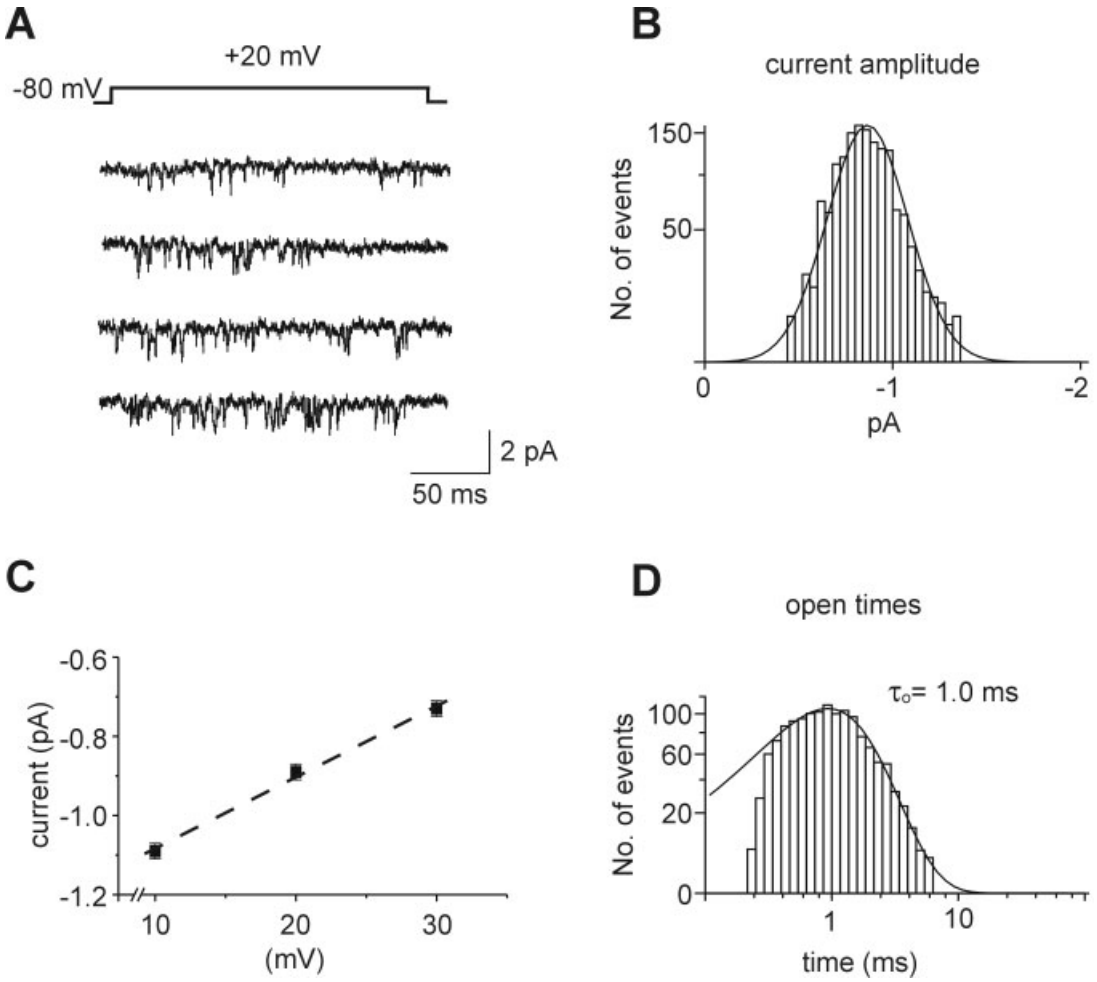

Fig. 4. Biophysical properties of N-type Ca^{2+} channels in cell-attached patches. **A:** Representative traces of N-channel activity during depolarization steps at 20 mV from $V_h = -80$ mV. Pipette solutions contained 5 μM nifedipine and 100 nM SNX-482. **B:** Distribution of N-current amplitudes at 20 mV. **C:** Slope conductance of N-channel measured by plotting current amplitudes at voltages ranging from 10 to 30 mV. **D:** Distribution of L-channel open times at 20 mV.

presence of L- and T-type channels that were expressed in response to specific stimuli. Barres et al. (1989, 1990) reported that astrocyte treatment with agents that increase intracellular cAMP levels promoted the expression and/or the activation of L-type Ca^{2+} channels, but no Ca^{2+} currents could be recorded in the absence of cAMP induction. They also found LVA (T-type) currents in a small percentage of cells but only when sera from some specific lots were added to the culture media. Coculture with neurons has also been suggested as an essential requisite for astrocyte expression of VGCCs (Corvalan et al., 1990).

In our study, none of these promoting factors appeared to be necessary for Ca^{2+} channel expression. Ca^{2+} currents were observed in 58% of the cells we examined, without any specific treatment. Our findings suggest that VGCCs are part of the normal ion channel outfit of cortical astrocytes, although their availability may be modulated by various physiological factors. In all probability, our figures underestimate the magnitude of Ca^{2+} currents flowing through astrocyte VGCCs since, in the purified cultures we used, the astrocytes were deprived of stimulating factors of neuronal origin. Under physiological conditions, i.e., when astrocytes are in close contact with neurons in the brain tissue, Ca^{2+} flux through VGCCs might be much greater than that observed in our experiments. Collectively, these observations suggest that VGCCs can play significant functional roles in regulating Ca^{2+} influx in astrocytes and, consequently, in all astrocyte cell functions that are regulated by Ca^{2+} signals.

L- (Ca_v1) channels were the predominant HVA Ca^{2+} channel type in a relatively small fraction (25%) of the astrocytes we studied. In the remaining cells, most of the current passed through N- ($Ca_v2.2$) and R- ($Ca_v2.3$) channels. Previous studies conducted in cultured glial cells failed to demonstrate the presence of N-channels (Puro et al., 1996). In hippocampal slices, Akopian et al. (1996) found CTx-GVIA-sensitive Ca^{2+} currents in nonneuronal cells that were assumed to be astrocytes based on indirect evidence of their glutamine synthetase immunoreactivity.

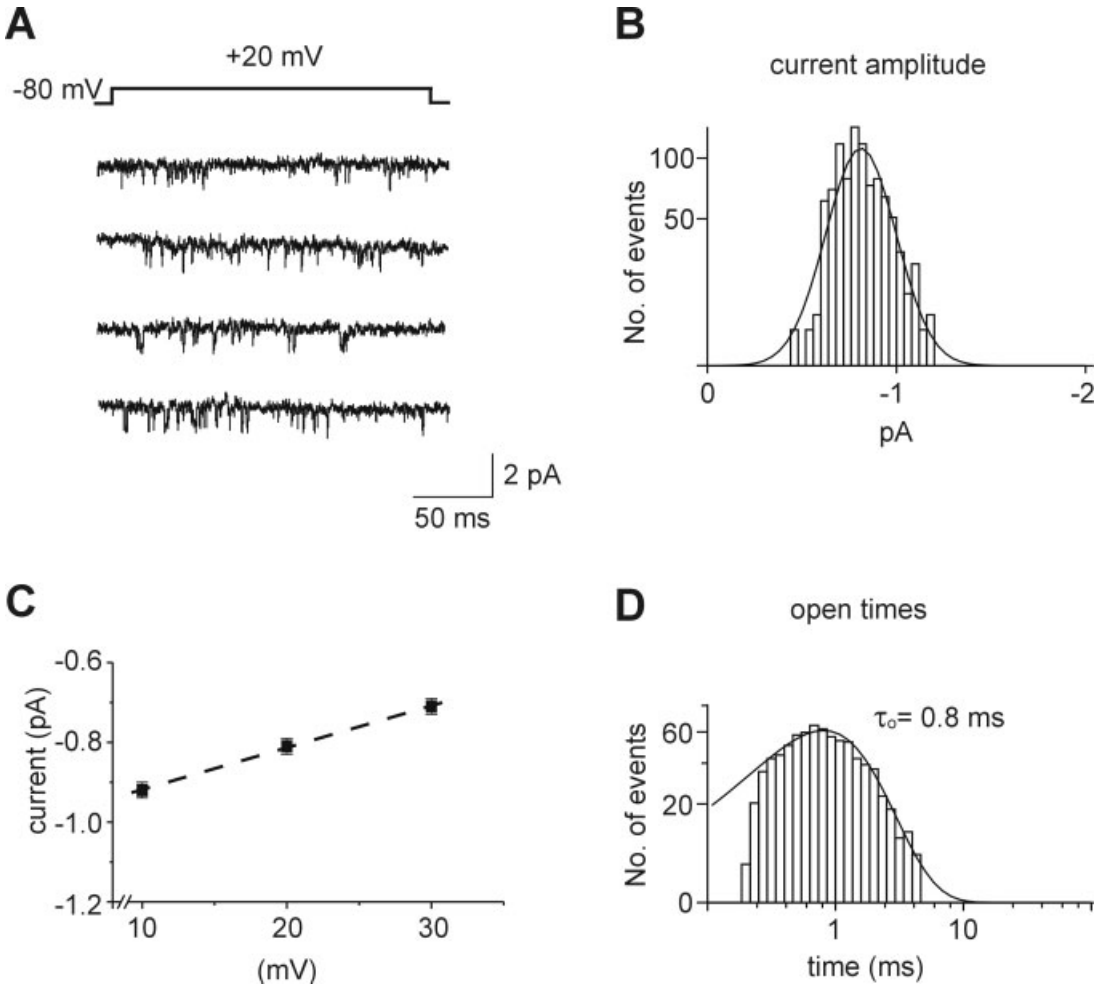

Fig. 5. Biophysical properties of R-type Ca^{2+} channels in cell-attached patches. **A:** Representative traces of R-channel activity during depolarization steps at 20 mV from $V_h = -80$ mV. Pipette solution contained 5 μM nifedipine and 10 μM CTx-MVIIC. Prior to recording, the cells were treated for 10 min with Tyrode's solution containing 3 μM CTx-GVIA and 10 μM CTx-MVIIC. **B:** Distribution of R-current amplitudes at 20 mV. **C:** Slope conductance of R-channel measured by plotting current amplitudes at voltages ranging from 10 to 30 mV. **D:** Distribution of R-channel open times at 10 mV.

In our experimental model, N-channel activity made a substantial contribution (33%) to the total recorded HVA current in astrocytes. In neurons, these channels play important roles in the calcium-mediated release of neurotransmitters (Catterall, 1998; Grassi et al., 1999; Spafford and Zamponi, 2003). Apart from mediating Ca^{2+} influx into the presynaptic terminal (like other HVA Ca^{2+} channels), the N-channels also interact with synaptic proteins responsible for active-zone docking of synaptic vesicles. It is thus possible that the N-channels we found in cortical astrocytes, and the other HVA channels as well, might be involved in the release of neurotransmitters stored in astrocytes, thus affecting the synaptic function. Astrocytes are equipped with transport systems for many neurotransmitters, and their parasynaptic processes are responsible for neurotransmitter uptake from the synaptic cleft (Kettenman and Ransom, 1995). Although astrocytes are nonexcitable cells, several stimuli are potentially capable of activating their VGCCs, including the increased extracellular K^+ concentrations that occur during repetitive nerve firing or the influx of Ca^{2+} and/or other cations through neurotransmitter-gated channels (Duffy and MacVicar, 1994; Latour et al., 2001).

To our knowledge, our study provides the first electrophysiological evidence of R- ($Ca_v2.3$) channels in glial cells and the first description of the biophysical properties of Ca_v1 (L-type), $Ca_v2.2$ (N-type), and $Ca_v2.3$ (R-type) in cortical astrocytes studied at the single-channel level. The unitary properties of these astrocyte VGCCs resemble those of neuronal L-, N-, and R-channels (Carabelli et al., 1996, 2002; Tottene et al., 1996; Elmsie, 1997; D'Ascenzo et al., 2002), providing further confirmation for our pharmacological characterization of macroscopic Ca^{2+} currents in these glial cells. The diversity of the VGCCs we observed, in terms of gating properties and voltage dependence, highlights the multiple modalities available to cortical astrocytes for regulating Ca^{2+} influx in response to different depolarizing stimuli occurring under different physiological conditions.

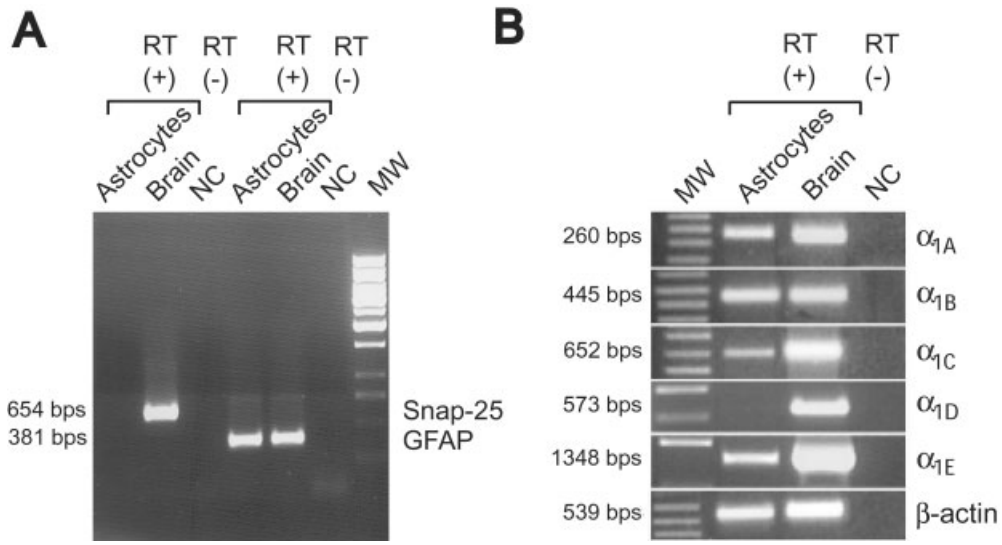

Fig. 6. RT-PCR analysis of mRNA for α_1 subunits expressed in rat astrocytes. The mRNA from astrocyte cell culture or rat brain tissue was reverse-transcribed into cDNA and (**A**) used as a template for PCR amplification of SNAP-25 and GFAP transcripts. **B:** The same samples were then used as a template for amplification of α_1 subunits with primers specific for the various classes of HVA Ca^{2+} channels. The amplification of β-actin fragment verifies the integrity and loading of cDNA samples. Size of PCR products is indicated to the left of each panel. MW, molecular weight marker (1 KB, Fermentas); brain, positive control; NC, negative control, i.e., amplification from astrocyte sample in absence of reverse transcription RT(−).

Our RT-PCR analysis revealed mRNA transcripts for the α_{1B}, α_{1C}, and α_{1E} subunits, which are the main components of N-, L-, and R-channels, respectively, as well as the α_{1A} subunit (P/Q channels). The latter observation was confirmed in repeat experiments, and the possibility that it was a result of neuronal contamination of our cultures was excluded by the absence of the neuronal marker SNAP-25 in the studied samples. However, no significant P/Q currents were observed in our electrophysiological experiments. While our study was in progress, similar results were published by Latour et al. (2003), who also found mRNA transcripts for subunits α_{1B}, α_{1C}, and α_{1E} in cultured astrocytes, as well as subunits α_{1D} and α_{1G}. Proteins for the corresponding Ca^{2+} channels were also detected in the astrocyte cell membranes by Western blot and immunocytochemistry. There was, however, no evidence of either subunit α_{1A} transcripts or P/Q channel proteins on the surfaces of the astrocytes. The discrepancies between these findings and ours, and the lack of agreement between our electrophysiological and molecular data relative to the P/Q channels, suggest that astrocytes are equipped to express all types of VGCCs but the actual realization of this potential is tailored to specific physiological conditions by factors that have yet to be identified.

In conclusion, our demonstration of different types of HVA Ca^{2+} channels in cultured astrocytes suggests that Ca^{2+} influx through VGCCs may play a fundamental role in producing Ca^{2+} signals in glial cells. Apart from regulating numerous glial cell functions, these signals may significantly contribute to the release of neurotransmitters stored in astrocytes. Astrocyte VGCCs are thus likely to play crucial roles in neuron-glia cross-talk through the modulating effects on synaptic transmission.

REFERENCES

Agrawal SK, Nashmi R, Fehlings MG. 2000. Role of L- and N-type calcium channels in the pathophysiology of traumatic spinal cord white matter injury. Neuroscience 99:179–188.

Akopian G, Kressin K, Derouiche A, Steinhäuser C. 1996. Identified glial cells in the early postnatal mouse hippocampus display different types of Ca^{2+} currents. Glia 17:181–194.

Araque A, Parpura V, Sanzgiri RP, Haydon PG. 1999. Tripartite synapses: glia, the unacknowledged partner. Trends Neurosci 22: 208–215.

Araque A, Li N, Doyle RT, Haydon PG. 2000. SNARE protein-dependent glutamate release from astrocytes. J Neurosci 20:666–673.

Attwell D. 1994. Glia and neurons in dialogue. Nature 369:707–708

Barres BA, Chun LL, Corey DP. 1989. Calcium current in cortical astrocytes: induction by cAMP and neurotransmitters and permissive effect of serum factors. J Neurosci 9:3169–3175.

Barres BA, Koroshetz WJ, Chun LL, Corey DP. 1990. Ion channel expression by white matter glia: the type-1 astrocyte. Neuron 5:527–544.

Bezzi P, Carmignoto G, Pasti L, Vesce S, Rossi D, Rizzini BL, Pozzan T, Volterra A. 1998. Prostaglandins stimulate calcium-dependent glutamate release in astrocytes. Nature 391:281–285.

Carabelli V, Lovallo M, Magnelli V, Zucker H, Carbone E. 1996. Voltage-dependent modulation of single N-type Ca^{2+} channel kinetics by receptor agonists in IMR32 cells. Biophys J 70:2144–2154.

Carabelli V, D'Ascenzo M, Carbone E, Grassi C. 2002. Nitric oxide inhibits neuroendocrine Ca_v1 L-channel gating via cGMP-dependent protein kinase in cell-attached patches of bovine chromaffin cells. J Physiol (Lond) 541:351–366.

Carmignoto G, Pasti L, Pozzan T. 1998. On the role of voltage-dependent calcium channels in calcium signaling of astrocytes in situ. J Neurosci 18:4637–4645.

Catterall WA. 1998. Structure and function of neuronal Ca^{2+} channels and their role in neurotransmitter release. Cell Calcium 24: 307–323.

Chung YH, Shin CM, Kim MJ, Cha CI. 2001. Enhanced expression of L-type Ca^{2+} channels in reactive astrocytes after ischemic injury in rats. Neurosci Lett 302:93–96.

Cornell-Bell AH, Finkbeiner SM, Cooper MS, Smith SJ. 1990. Glutamate induces calcium waves in cultured astrocytes: long-range glial signaling. Science 247:470–473.

Corvalan V, Cole R, de Vellis J, Hagiwara S. 1990. Neuronal modulation of calcium channel activity in cultured rat astrocytes. Proc Natl Acad Sci USA 87:4345–4348.

D'Ascenzo M, Martinotti G, Azzena GB, Grassi C. 2002. cGMP/protein kinase G-dependent inhibition of N-type Ca^{2+} channels induced by nitric oxide in human neuroblastoma IMR32 cells. J Neurosci 22: 7485–7492.

Duffy S, MacVicar BA. 1994. Potassium-dependent calcium influx in acutely isolated hippocampal astrocytes. Neuroscience 61:51–61.

Elmslie KS. 1997. Identification of single channels which underlie the N-type and L-type calcium current in bullfrog sympathetic neurons. J Neurosci 17:2658–2668.

Grassi C, Martire M, Altobelli D, Azzena GB, Preziosi P. 1999. Characterization of Ca^{2+} channels responsible for K^+-evoked [^{3}H]noradrenaline release from rat brain cortex synaptosomes and their response to amyotrophic lateral sclerosis IgGs. Exp Neurol 159: 520–527.

Hamill OP, Marty A, Neher E, Sakmann B, Sigworth FJ. 1981. Improved patch-clamp techniques for high-resolution current recording from cells and cell-free membrane patches. Pflügers Arch 391: 85–100.

Haydon PG. 2001. Glia: listening and talking to the synapse. Nat Rev Neurosci 2:185–193.

Kettenmann H, Ransom BR. 1995. Neuroglia. New Yor: Oxford University Press.

Latour I, Gee CE, Robitaille JC. 2001. Differential mechanisms of Ca^{2+} responses in glial cells evoked by exogenous and endogenous glutamate in rat hippocampus. Hippocampus 11:132–145.

Latour I, Hamid J, Beedle AM, Zamponi GW, Macvicar BA. 2003. Expression of voltage-gated Ca^{2+} channel subtypes in cultured astrocytes. Glia 41:347–353.

Leybaert L, Paemeleire K, Strahonja A, Sanderson MJ. 1998. Inositol-trisphosphate-dependent intercellular calcium signaling in and between astrocytes and endothelial cells. Glia 24:398–407.

MacVicar BA. 1984. Voltage-dependent calcium channels in glial cells. Science 226:1345–1347.

MacVicar BA, Tse FWY. 1988. Norepinephrine and cyclic adenosine 3′:5′-cyclic monophosphate enhance a nifedipine-sensitive calcium current in cultured rat astrocytes. Glia 1:359–365.

MacVicar BA, Hochman D, Delay MJ, Weiss S. 1991. Modulation of intracellular Ca^{2+} in cultured astrocytes by influx through voltage-activated Ca^{2+} channels. Glia 4:448–455.

McCarthy KD, de Vellis J. 1980. Preparation of separate astroglial and oligodendroglial cell cultures from rat cerebral tissue. J Cell Biol 85:890–902.

Parpura V, Basarsky TA, Liu F, Jeftinija K, Jeftinija S, Haydon PG. 1994. Glutamate-mediated astrocyte-neuron signalling. Nature 369:744–747.

Parpura V, Haydon PG. 2000. Physiological astrocytic calcium levels stimulate glutamate release to modulate adjacent neurons. Proc Natl Acad Sci USA 97:8629–8634.

Pfrieger F, Barres BA. 1997. Glial cells regulate synaptic efficacy. Science 277:1684–1687.

Puro DG, Hwang JJ, Kwon OJ, Chin H. 1996. Characterization of an L-type calcium channel expressed by human retinal Muller (glial) cells. Mol Brain Res 37:41–48.

Rae J, Cooper K, Gates P, Watsky M. 1991. Low access resistance perforated patch recordings using amphotericin B. J Neurosci Meth 37:15–26.

Spafford JD, Zamponi GW. 2003. Functional interactions between presynaptic calcium channels and the neurotransmitter release machinery. Curr Opin Neurobiol 13:308–314.

Tottene A, Moretti A, Pietrobon D. 1996. Functional diversity of P-type and R-type calcium channels in rat cerebellar neurons. J Neurosci 16:6353–6363.

Ullian, EM, Sapperstein SK, Christopherson KS, Barres BA. 2001. Control of synapse number by glia. Science 291:657–661.

Vairano M. Dello Russo C, Pozzoli G, Battaglia A, Scambia G, Tringali G, Aloe-Spiriti MA, Preziosi P, Navarra P. 2002. Erythropoietin exerts anti-apoptotic effect on rat microglial cells in vitro. Eur J Neurosci 16:584–592.

Verkhratsky A, Orkand RK, Kettenmann H. 1998. Glial calcium: homeostasis and signaling function. Physiol Rev 78:99–141.

Verkhratsky A, Steinhäuser C. 2000. Ion channels in glial cells. Brain Res Brain Res Rev 32:380–412.

Westenbroek RE, Bausch SB, Lin RC, Franck JE, Noebels JL, Catterall WA. 1998. Upregulation of L-type Ca^{2+} channels in reactive astrocytes after brain injury, hypomyelination, and ischemia. J Neurosci 18:2321–2334.